

Study of bottom production via its semi-leptonic decay with the STAR Heavy Flavor Tracker

Yifei ZHANG^{1,2}, Jonathan BOUCHET³, Xin DONG²,
Spyridon MARGETIS³, Hans Georg RITTER²

¹*University of Science and Technology of China, Hefei, Anhui, 230026 China*

²*Lawrence Berkeley National Laboratory, Berkeley, CA, 94720 USA*

³*Kent State University, Kent, Ohio, 44242 USA*

Abstract

We explore the possibility of identifying the B-meson through its semi-leptonic decay $B \rightarrow e + X$ with the STAR Heavy Flavor Tracker. We present a method to separately measure charm and beauty ~~from their decay mi~~, the non-photonic ~~electrons~~, by exploring the different impact parameters of ~~the~~ decay electrons. The errors of the transverse momentum distributions, nuclear modification factors and elliptic flow parameters of the electrons from heavy flavor decay are estimated ~~in the RHIC environment~~. Relevant physics topics are discussed.


Key words: charm, bottom, semi-leptonic decay, Heavy Flavor Tracker.

1 Introduction

In central Au+Au collisions at the Relativistic Heavy Ion Collider (RHIC), light quark (u, d) hadrons and away-side back-to-back jets are strongly suppressed compared to the yields in $p + p$ collisions [1]. Light quarks experience a large energy loss when traversing the hot dense matter created in the nuclear nuclear collisions. The elliptic flow parameter v_2 of light quark or strange quark (s) hadrons as a function of transverse momentum (p_T) obeys number of quark scaling, successfully described by quark coalescence models [2]. This indicates the formation of hot dense matter with partonic collectivity in heavy ion collisions [3].

Charm and beauty quarks are much heavier ($m_c \simeq 1.3 \text{ GeV}/c^2$, $m_b \simeq 4.8 \text{ GeV}/c^2$) than light quarks and they will maintain their mass during strong

interactions in the QCD vacuum. They are produced at an early stage of the collision and their production can be evaluated by perturbative QCD [4,5]. Therefore, their production cross sections in nuclear collisions are found to scale with the number of binary nucleon-nucleon collisions [6]. Heavy quarks are a unique tool to probe the properties of strongly interacting matter created in relativistic heavy ion collisions.

The dead-cone effect predicts that heavy quarks lose less energy than light quarks by gluon radiation when they traverse a Quark-Gluon Plasma (QGP) [7], and this is especially true for bottom quarks. Even when  elastic energy loss is included, bottom quark still lose less energy [8,9]. ~~In contrast,~~ recent measurements of non-photonic electrons (NPE) from heavy quark decays at high transverse momentum show similar suppression to that of the light hadrons [10]. This observation challenges understanding of the heavy quark energy loss mechanisms and pf how heavy quarks interact with the hot dense medium. Precise measurements of charm and bottom quark energy loss separately is crucial for understanding the heavy quark energy loss mechanisms.

Recently, PHENIX has measured the non-photonic electron v_2 [11]. The observed large elliptic flow of the non-photonic electrons may indicate strong coupling of heavy quarks with the medium. Heavy quarks may flow as a result of frequent interactions with light quarks in a dense medium. Light quarks then are likely to approach thermal equilibrium. In particular, bottom quarks are not very likely to flow due to their extremely heavy mass. The angular correlation between bottom hadron and its decay electron is weak at low and intermediate p_T (< 3 GeV/ c). Even if charm hadrons and bottom hadrons have similar v_2 values, the v_2 of electrons from bottom hadron decays is much smaller than that from charm decays [12]. Thus, the v_2 measurement at low p_T of electrons from charm and bottom decays is as an important probe to test the thermalization of the QGP. Comparing with models like heavy quark and light quark coalescence [13], measurements of heavy quark v_2 at intermediate p_T impact on our understanding of the participance of heavy quarks in the partonic collectivity at the early stage of the collisions.

At RHIC first attempts have been made to separate charm and beauty contributions to non-photonic electrons from heavy flavor decays [14], but the current detectors do not have sufficient resolution for precision measurements. The STAR Heavy Flavor Tracker (HFT) is designed to significantly extend the physics reach of the STAR experiment for precise measurements of heavy quarks [15]. The HFT consists of 4 concentric layers of silicon detectors. The outermost layer at 22 cm is a silicon strip detector (SSD), the next layer consists of the Intermediate Silicon Tracker (IST) at 14 cm. The inner two layers at 8 cm and at 2.5 cm are done in pixel technology [15]. The PIXEL detector is composed of two layers of monolithic CMOS Active Pixel sensors [17] which measure the position of a particle hit with a resolution of 8.6 microns in both

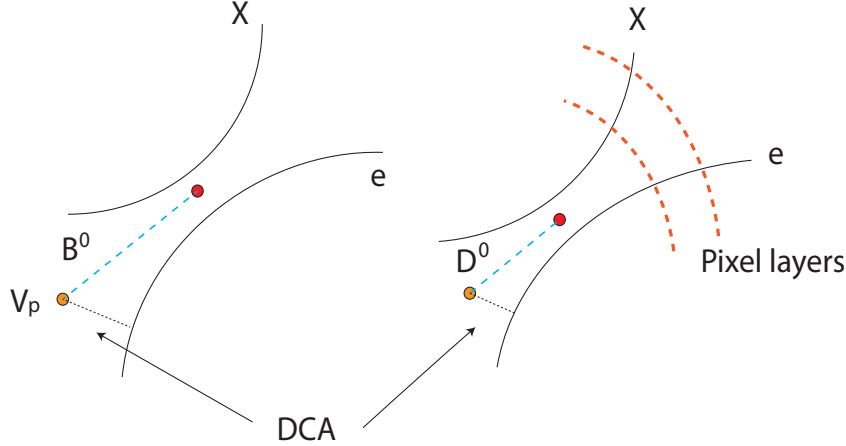


Fig. 1. The difference of the DCA of daughter electrons from D^0 and B^0 semi-leptonic decays.

R/ ϕ and Z direction. The total HFT material budget is less than 3% radiation length (X_0), while PIXEL detector is only 0.37% X_0 per layer, which provides great advantage to reduce electron background from photon conversion. The SSD and IST are designed to link tracks found in the STAR Time Projection Chamber (TPC) to the PIXEL detector.

2 Method

The B-meson through its semi-leptonic decay $B \rightarrow e + X$ can be separated from D-mesons by exploring the large impact parameter of the decay electrons with respect to the collision vertex. One has the choice of either subtracting the D contribution from the total NPE signal or trying to separate the signal by exploring the difference in lifetime (thus in impact parameter). We utilize the impact parameter method to separate electrons of B decays from those from D decays. Since B mesons have mean proper decay lengths of about $500 \mu\text{m}$, their decay electrons are characterized by large distance of closest approach (DCA) to the collision vertex. The STAR HFT provides a good resolution of track DCA ($\sigma_{DCA} \sim 20 \mu\text{m}$ for $p_T \geq 2 \text{ GeV}/c$). A cut imposing a minimum value of DCA rejects a large fraction of the electrons from light meson decays and photon conversions, as well as primary pions misidentified as electrons. For central Au+Au collisions the reconstructed event vertex resolution is $\sim 3 \mu\text{m}$ in the $r - \phi$ and z coordinates, which provides the precision to distinguish the DCA to the primary vertex of the electrons from different heavy flavor mesons (D, B) semi-leptonic decays due to their different lifetime, shown in Fig. 1.

The D^0 , D^+ , B^0 , B^+ , were embedded flat in p_T (0.2-20 GeV/c) in Hijing central Au+Au events. The pseudo-rapidity is flat in ± 1 units around mid-rapidity and flat in azimuth. The p_T spectra were weighted using STAR mea-

Particles	$c\tau$ (μm)	Mass (GeV/c^2)	$q(c, b) \rightarrow X$ (FR)	$X \rightarrow e$ (BR)
D^0	123	1.865	0.565	0.0653
D^+	312	1.869	0.246	0.160
B^0	459	5.279	0.40	0.101
B^+	491	5.279	0.40	0.108

Table 1
 PDG numbers of D, B mesons.

sured D^0 spectrum power-law distribution for D mesons and FONLL calculations for B mesons [6]. D^0 and D^+ were forced to decay semileptonically ($D^0, D^+ \rightarrow e + X$) with 100% branching ratio. Since B^0 and B^+ are very similar in this simulation, we will use B to represent both of them. B mesons decay 75% to semi-leptonic channel ($B \rightarrow e + D^* + X$) and 25% to semi-leptonic channel ($B \rightarrow e + D + X$). The fraction of the process $B \rightarrow D^* \rightarrow D \rightarrow e$ is relatively small, we only simulate $B \rightarrow e + X$ and $B \rightarrow D \rightarrow e$. All these channels are later scaled by the fragmentation ratio (FR) and branching ratio (BR) in the final analysis. Table 1 lists the $c\tau$, mass, FR and BR for these particles [18].

Due to larger $c\tau$, the DCA distribution of electrons from B decay is expected to be broader than that of $D^0 \rightarrow e$. Since D^+ $c\tau$ is closer to that of B mesons, it becomes a challenge to distinguish them by electron DCA distributions only. However, the D^+ reconstruction via hadronic decay (e.g. $D^+ \rightarrow K\pi\pi$) can provide a precise constraint on p_T distributions of the decay electrons. Thus together with the electron DCA distributions, we will be able to separate D and B meson production with the HFT. The HFT has a good electron reconstruction efficiency. Fig. 2 shows the electron tracking efficiency with the requirement of two hits in the pixel layers. We included here a 85% acceptance and tracking efficiency in the TPC.

For particle identification we used the time of flight (TOF) detector for low p_T and the barrel calorimeter (BEMC) for high p_T and a realistic energy loss (dE/dx) in the TPC [1]. Good electron candidates were selected with a number of total fit points > 15 (out of 45), pseudo-rapidity in ± 1 , and with two pixel hits required on the track in the TPC. All electrons from photon conversions outside of the pixel detector can be removed with this requirement. The main background sources in this analysis are electrons from photon conversions in the beam pipe and part of the first pixel layer and electrons from π^0 and η Dalitz decays. We embedded π^0 s with flat p_T in the simulation events with the same branching ratio 50% for conversion and Dalitz. The p_T distributions were weighted by the PHENIX π^0 spectrum [19]. From the photonic to inclusive electron ratio measured in STAR [6], the background of photon conversions

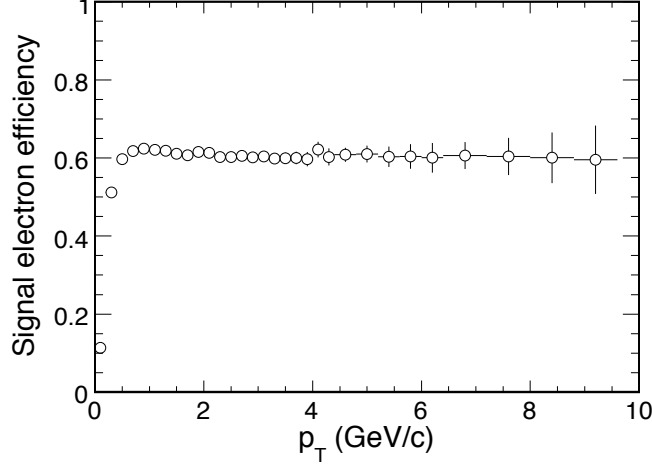


Fig. 2. Efficiency of electron in the STAR TPC+HFT tracking.

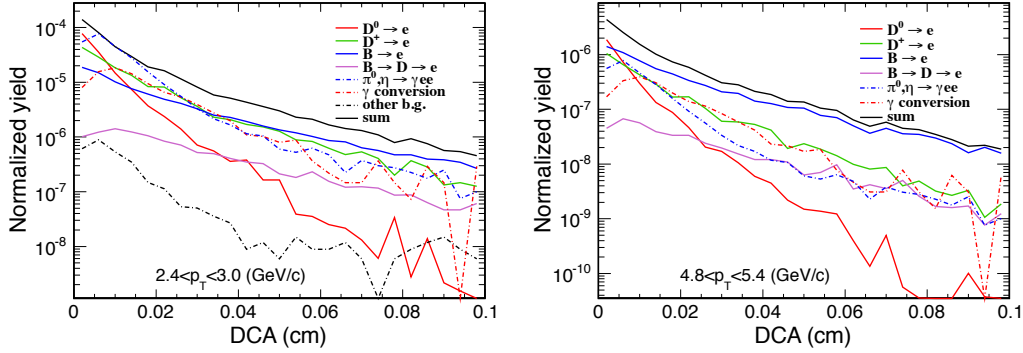


Fig. 3. The electron DCA distributions for D and B meson semi-leptonic decay for two different p_T regions.

and Dalitz decays can be scaled to the STAR condition in future runs. The background from other hadron decays overall is small and negligible at high p_T . We assume that the background p_T is decreasing exponentially and use this to extrapolate to empty bins at higher p_T . The electron DCA distributions from different decay processes were normalized by the corresponding FR and BR in Table 1, and the total electron yield was normalized to STAR measured non-photonic electron (NPE) spectrum [?]. The ($B \rightarrow e$) over NPE ratio was normalized to fit the STAR data from e-h correlation measurements [21]. Fig. 3 shows the electron DCA distributions at $2.4 < p_T < 3$ GeV/c (left panel) and at $4.8 < p_T < 5.4$ GeV/c (right panel) for $D^0 \rightarrow e$ (red), $D^+ \rightarrow e$ (green), $B \rightarrow e$ (blue) and $B \rightarrow D \rightarrow e$ (purple). The dot-dashed curves are for background DCA distributions. The black solid curve presents the total electron DCA distribution, which was normalized to the STAR measured NPE spectrum.

3 Results

We use the individual DCA distributions to fit the total DCA distribution in order to extract the raw yield of each source of electrons statistically. The p_T distributions of D meson, especially D^+ , from our measurements via hadronic decay channel will constrain the $D \rightarrow e$ distributions [15]. By subtracting the $D \rightarrow e$ DCA distributions in each p_T bin from the total DCA distribution, the electrons from B meson decays can be obtained.

Figure 4 shows the $D \rightarrow e$, $B \rightarrow e$ and $B \rightarrow D \rightarrow e$ spectra. The statistical uncertainties were estimated for 500M minimum bias Au+Au events. The background from gamma conversion, π^0 , η Dalitz and other hadron decays are shown as dashed, dotted and dot-dashed curves, respectively. The systematic uncertainties for $B \rightarrow e$ from subtraction of D-meson p_T spectra reconstructed via hadronic channels are estimated as yellow and cyan bars for central 0-10% events and 0-80% minimum bias events, respectively. Constrained by the measurement of D-meson hadronic decays, the precise measurement of electron spectra from D and B decays separately will allow to extract the bottom cross section.

Figure 5 shows the ratio of the number of electrons from bottom decay to the number of electrons from charm and bottom decay as a function of p_T . The blue lines represent the band of uncertainty of FONLL calculations [5]. Open stars show preliminary results for 200 GeV p+p collisions measured by STAR [21]. Both theory calculations and experiments show large uncertainties. However, with the STAR HFT the ratio will be measured with great precision. For low p_T the ratio and the expected errors are calculated from 50M Au+Au central events (open circles). For high p_T we used a high tower (HT) trigger sampling 500 μb^{-1} luminosity (filled circles). Since the ratio is obtained directly from the measured electron spectra from D and B decays with HFT, there is no model dependent and the systematic errors will be greatly reduced compared with the data from electron-hadron correlations.

Fig. 6 shows the estimated precision for a measurement of R_{CP} of electrons from D (red circles) and B (blue squares) decays as a function of p_T , where we assume the respective R_{CP} (dotted curves) from a theoretical calculation of the T-matrix approach to heavy quark diffusion in the QGP [22]. For low p_T , R_{CP} and the expected errors are calculated from 500M Au+Au central events (open symbols). For high p_T we used a high tower trigger sampling 500 μb^{-1} luminosity (filled symbols). Apparently, with the STAR HFT the R_{CP} of electrons from D and B decays can be well separated and measured. This is very important for understanding the heavy flavor energy loss mechanisms and will provide a constraint for theory calculations.

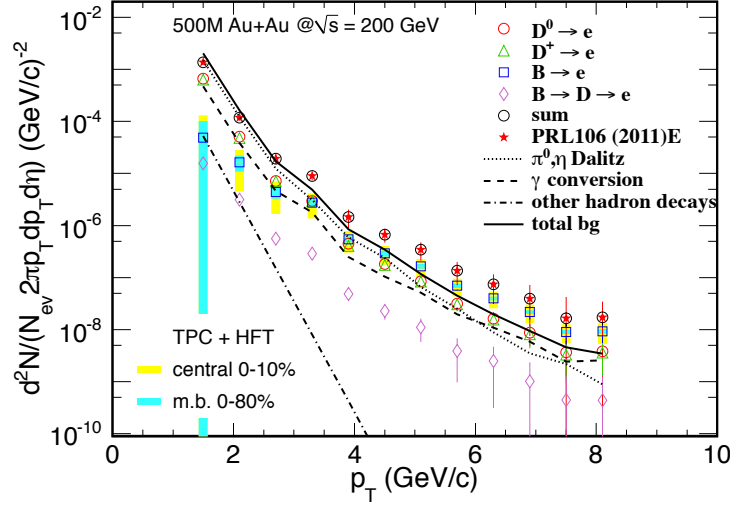


Fig. 4. Electron spectra from B and D meson semi-leptonic decay. The expected errors as a function of p_T were estimated for 500M Au+Au minimum bias events. Estimated main background sources are shown in curves. The systematic uncertainties for $B \rightarrow e$ from subtraction of D-meson p_T spectra reconstructed via hadronic channels are estimated as yellow and cyan bars for central 0-10% events and 0-80% minimum bias events, respectively.

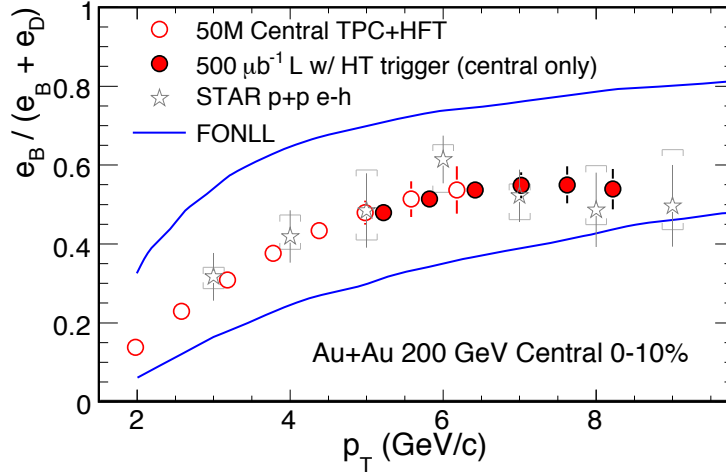


Fig. 5. The $(B \rightarrow e)/NPE$ ratio as a function of p_T . Expected errors are estimated for 50M Au+Au central events (open circles) and $500 \mu b^{-1}$ sampled luminosity with a high tower trigger (filled circles). Open stars represent preliminary results from 200 GeV p+p collisions.

We can use a variational method to measure the elliptic flow parameter of electrons for both $D \rightarrow e$ and $B \rightarrow e$ following the equation:

$$v_2^{NPE} = r \times v_2^{B \rightarrow e} + (1 - r) \times v_2^{D \rightarrow e}, \quad (1)$$

Here r is the $(B \rightarrow e)/NPE$ ratio. The value of r can be varied by applying

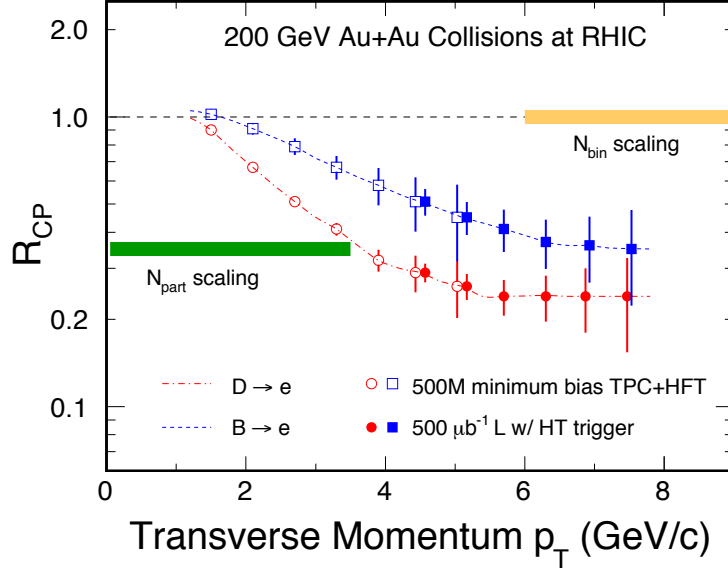


Fig. 6. Nuclear modification factor R_{CP} of electrons from D meson and B meson decays. Expected errors are estimated for 500M Au+Au minimum bias events (open symbols) and 500 μb^{-1} sampled luminosity with a high tower trigger (filled symbols).

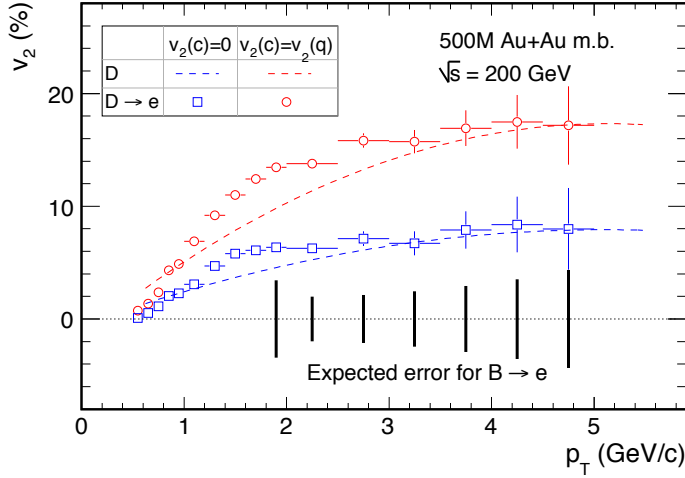


Fig. 7. Expected statistical errors of $D \rightarrow e$ and $B \rightarrow e$ v_2 for 500M Au+Au minimum bias events.

different DCA cuts. From the v_2 of the non-photonic electrons from different DCA cuts we can extract the electron v_2 for both, $D \rightarrow e$ and $B \rightarrow e$. We also will have a precise measurement of the v_2 of D mesons as a function of p_T via reconstruction from the hadronic decay channel [15], which constrains the $D \rightarrow e$ v_2 due to decay kinematics. Thus the v_2 of B mesons decaying into electrons can be obtained.

In order to estimate statistics of the electron v_2 measurement we assume that the v_2 of D mesons follows a transport model with quark coalescence [23] and

does not drop at high p_T . The red dashed curve in Fig. 7 shows the D meson v_2 for the case that the charm quark has the same size partonic flow as measured for the light quarks ($v_2(c)=v_2(q)$). The blue dashed curve shows the limiting case where the charm quark does not flow ($v_2(c)=0$). We use the form factor decay [24] to generate $D \rightarrow e v_2$ distributions, shown as red open circles and blue open squares for the corresponding two cases. The ratio $r = (B \rightarrow e)/NPE$ is taken from STAR e-h correlation shown in Fig. 5. The v_2 of non-photon decay electrons is taken from the PHENIX measurement [11]. The $B \rightarrow e v_2$ can be obtained from equation 1. The statistic errors shown in Fig. 7 are estimated for both, $D \rightarrow e v_2$ (red and blue bars) and $B \rightarrow e v_2$ (black bars), with 500M Au+Au minimum bias events. A possible Λ_c enhancement in Au+Au is not taken into account in the v_2 estimate.

In summary, we present a method to measure mesons containing bottom quarks through their semi-leptonic decays. The STAR HFT is designed to distinguish the impact parameters of the electrons from D and B meson decays. We estimated the expected precision for the electron spectra, R_{CP} and v_2 from D and B meson decays in the future with STAR low material environment. This will provide precise experimental results for understanding the energy loss of heavy quarks, flow properties and their interactions with the hot dense medium created in heavy-ion collisions at RHIC.

We thank the STAR-HFT group, the NERSC Center at LBNL for their support. This work was supported in part by the Offices of NP and HEP within the U.S. DOE Office of Science, and the National Natural Science Foundation of China (NSFC) with grant No. 10805046.

References

- [1] J. Adams *et al.*, Nucl. Phys. A 757 (2005) 102.
- [2] D. Molnar and S.A. Voloshin, Phys. Rev. Lett. 91 (2003) 092301.
- [3] B. I. Abelev *et al.*, Phys. Rev. C 77 (2008) 54901.
- [4] Z. Lin and M. Gyulassy, Phys. Rev. C 51 (1995) 2177.
- [5] M. Cacciari, P. Nason and R. Vogt, Phys. Rev. Lett. 95 (2005) 122001.
- [6] J. Adams *et al.*, Phys. Rev. Lett. 94 (2005) 062301; Y. Zhang, J. Phys. G 32 (2006) S529; B. I. Abelev, *et al.*, arXiv: 0805.0364. B. I. Abelev *et al.*, Phys. Rev. Lett. 106 (2011) 159902(E).
- [7] Yu. L. Dokshitzer and D.E. Kharzeev, Phys. Lett. B 519 (2001) 199; M. Djordjevic, M. Gyulassy and S. Wicks, Phys. Rev. Lett. 94 (2005) 112301; N. Armesto, A. Dainese, C.A. Salgado and U.A. Wiedemann, Phys. Rev. D 71 (2005) 054027.

- [8] M. Djordjevic, M. Gyulassy, R. Vogt and S. Wicks, Phys. Lett. B 632 (2006) 81.
- [9] R. Rapp and H. Hees, J. Phys. G 32 (2006) S351.
- [10] S. S. Adler *et al.*, Phys. Rev. Lett. 96 (2006) 032301.
- [11] S. S. Adler *et al.*, Phys. Rev. Lett. 98 (2007) 172301; D. Hornback, J. Phys. G 35 (2008) 104113.
- [12] Y. Zhang, Nucl. Phys. A 783 (2007) 489c.
- [13] H. Hees, V. Greco and R. Rapp, Phys. Rev. C 73 (2006) 034913.
- [14] A. Adare *et al.*, Phys. Rev. Lett. 103 (2009) 082002. M. M. Aggarwal *et al.*, arXiv: 1007.1200.
- [15] J. Kapitan, Eur. Phys. J. C 62 (2009) 217; J. Bouchet, Nucl. Phys. A 830 (2009) 636c-637c.; Z. Xu *et al.*, J. Phys. G 32 (2006) S571.
- [16] R. Bellwied, *et al.*, Nucl. Instrum. Meth. A 499 (2003) 652.
- [17] E. Anderssen, *et al.*, Technique Note,
<http://www.osti.gov/bridge/servlets/purl/939892-be12Up/939892.pdf>.
- [18] W. M. Yao *et al.*, J. Phys. G 33 (2006) 1.
- [19] S. S. Adler *et al.*, Phys. Rev. C 76 (2007) 034904.
- [20] S. S. Adler *et al.*, Phys. Rev. C 75 (2007) 024909.
- [21] S. Sakai *et al.*, J. Phys. G 36 (2009) 064056.
- [22] H. van Hees *et al.*, Eur. Phys. J. C 61 (2009) 799.
- [23] V. Greco, C. M. Ko, and R. Rapp, Phys. Lett. B 595 (2004) 202.
- [24] H. D. Liu *et al.*, Phys. Lett. B 639 (2006) 441.